



Analytical Methods

A precise and efficient detection of Beta-Cyfluthrin via fluorescent molecularly imprinted polymers with ally fluorescein as functional monomer in agricultural products



Hao Qiu, Lin Gao, Jixiang Wang, Jianming Pan, Yongsheng Yan*, Xifeng Zhang*

School of Chemistry and Chemical Engineering, Jiangsu University, Zhenjiang 212013, People's Republic of China

ARTICLE INFO

Article history:

Received 29 August 2015

Received in revised form 13 May 2016

Accepted 5 September 2016

Available online 8 September 2016

Keywords:

Fluorescent molecularly imprinted polymers

Beta-Cyfluthrin

Fluorescence detection

ABSTRACT

In this study, an effective and precise fluorescent molecularly imprinted polymers (FMIPs) for the determination of Beta-Cyfluthrin (BC) was synthesized via precipitation polymerization with SiO₂ as the carrier, BC as the target molecule, ally fluorescein as the functional monomer, trimethylolpropane trimethacrylate (TRIM) as the crosslinker. Moreover, the characteristic of material has been measured by FTIR, TEM, SEM, TGA, LSCM and fluorescence spectrophotometer. Average diameter and shell thickness of as-synthesized microspheres were 300 nm and 50 nm, respectively. An excellent linear relationship of SiO₂-MPTMS@FMIPs with a correlation coefficient of 0.9919 could be gained covering a wide concentration range of 10.11–80 nM described by the Stern-Volmer equation. The limit of detection (LOD) was evaluated with the equation $LOD = 3\sigma/S$ and was found to be 10.11 nM. The study demonstrated that SiO₂-MPTMS@FMIPs could improve the determination for BC and illustrated the good prospects of SiO₂-MPTMS@FMIPs for BC detection in agricultural products.

© 2016 Elsevier Ltd. All rights reserved.

1. Introduction

Pyrethroids as a class of pesticide of artificial synthesis whose structure is similar to imitative natural chrysanthemum ester have been widely used for control of animals and agriculture, even in household application (Chalányová, Paulechová, & Hutta, 2006) owing to excellent fast-acting property, enhanced insecticidal activity, broad spectrum, low toxicity and low residue. In the past study, pyrethroids were found that they had low toxicity for humans and mammals, not representing that it was not harmless for human. However, it was extremely harmful for aquatic animal, particularly fish and shrimp. Beta-Cyfluthrin (BC), cyano (4-fluoro-3-phenoxyphenyl) methyl 3-(2,2-dichloroethenyl)-2,2-dimethylcy clopropanecarboxylate as an optical isomer of cyfluthrin has four diastereoisomeric pairs of enantiomers. However, the toxicity of BC is approximately 2–5 times higher than that of cyfluthrin (European Commission, 2002). That is to say, people may be in danger during the process of producing or utilizing, even threatened by pest control operation, contaminated agricultural products and water and so on. Therefore, much time and many efforts were spent to discover a kind of rapid, sensitive and efficient method for determining pesticides residual in agricultural products.

In recent decades, several efficient methods for determining pyrethroids have been discovered, mainly including gas chromatography (GC) (Dalluge, Beens, & Brinkman, 2003; Holmstead & Fullmer, 1977; Lehotay, Lightfield, Harman-Fetcho, & Donoghue, 2001), high-performance liquid chromatography (HPLC) (Hamscher, Sczesny, Hoper, & Nau, 2002; Katagi, 1991, 1993), and thin-layer chromatography (TLC) (Cimpoiu, Hosu, & Hodisan, 2006; Griesinger et al., 2014; Lv, Lin, Tan, & Svec, 2013). Galera and co-workers have found an efficient method to determine BC by HPLC with post-column photoderivatization (Galera, Garcia, & Valverde, 2006). A rapid and efficient scheme has been developed via matrix solid phase dispersion (MSPD) combined with liquid chromatography (LC) with ultraviolet diode array detector for determination of BC in stem of coconut palm (Ferreira et al., 2013).

Molecular imprinting technique (MIT) (Alexander et al., 2003; Andersson, 2000; Masqueè, Marceè, & Borruil, 2001; Ye & Mosbach, 2008) which provides a promising peculiar way to deliver specific molecular recognition elements with highly selectivity, sensitivity and low cost has been widely utilized in analysis and detection. Molecularly imprinted polymers (MIPs) which is in copolymerization of the functional monomers, cross-linkers and template molecules can be synthesized (Chen, Xu, & Li, 2011). Pan et al. have synthesized magnetic molecularly imprinted polymers (MMIPs) for selective recognition of 2,4-dichlorophenol

* Corresponding authors.

E-mail addresses: yys@mail.ujss.edu.cn (Y. Yan), qhujss17@126.com (X. Zhang).

(2,4-DCP) (Pan et al., 2011). Li and co-workers have studied adsorption of dansylated amino acids based on molecularly imprinted surfaces (Li & Husson, 2006). Jing and co-workers have synthesized molecularly imprinted nanoparticles based on magnetic composites with selective recognition of lysozyme (Jing et al., 2010). Obviously, compared with the traditional methods of separation based on selective adsorption, the advantages of excellent selective recognition, simple technological and good reproducibility are exposed. MIPs have aroused extensive attention and been widely applied in many other fields because of these excellent properties, such as solid-phase extraction, chemical sensors and artificial antibodies (Chen et al., 2011; Haupt & Mosbach, 2000; He, Long, Pan, Li, & Liu, 2007; Piletsky et al., 2000). Caro et al. have studied the application of molecularly imprinted solid-phase extraction (MISPE) to compounds from environmental and biological samples (Caro, Marce', Borrull, Cormack, & Sherrington, 2006). Ma and Chen have successfully synthesized a kind of magnetic molecularly imprinted polymers (MMIPs) using carbon nanotubes as matrix to separate and recognize pyrethroids (Ma & Chen, 2014). Shi et al. determined six pyrethroid insecticides including BC by molecularly imprinted solid phase extraction combined with gas chromatography (GC-MISPE) (Shi, Liu, Sun, Li, & Chen, 2012).

In recent years, the fluorescence detection method has increasingly attracted public attention due to the characteristic of high efficiency, simplicity and sensitivity, compared with traditional detection method. Therefore, we hope to combine molecular imprinting technique with the fluorescence detection to enhance the advantages of accurate recognition and capture ability of MIPs to make template molecules be selectively absorbed on surface of MIPs. Via bringing in fluorescence detection, the consequence of the detection can be intuitively observed and a fast and efficient test to detect template molecules can be easily carried out, which was observed via fluorescence intensity curves. Therefore, fluorescent monomer is added during the synthetic process and the fluorescence intensity will quench after the reaction of template molecules and MIPs (Lakowicz, 2005). Ge and co-workers have synthesized highly fluorescent silica molecularly imprinted nanoparticles embedded CdTe quantum dots (CdTe-SiO₂-MIPs) as a novel deltamethrin sensor (Ge, Lu, Ge, Yan, & Yu, 2011). Ng and Narayanaswamy have synthesized the fluorescence sensor using a molecularly imprinted polymer as a recognition receptor for the detection of aluminium ions in aqueous media (Ng & Narayanaswamy, 2006). Gao and co-workers have presented a efficient protocol for synthesizing the fluorescent molecularly imprinted polymers to detect cyhalothrin in honey via precipitation polymerization (Gao et al., 2014). Advantages and disadvantages compared with traditional methods were shown in Table 1. Compared with other detection methods, this method had the advantages of high sensitivity, simplicity, efficiency, low LOD and speed, which the process of detection only spent 1–2 min. However, the detecting technology was immaturity and boundedness, which only apply to materials with fluorescent properties. Therefore, it should be further investigated in detail.

As is well-known that traditional fluorescent molecular imprinting technique is that composite is performed utilizing the covalent and non-covalent interaction between target molecular and functional monomer, then fluorescent dye is grafted into MIPs. Traditional functional monomer includes methacrylic acid (MAA), Methyl methacrylate (MMA), acrylamide (AM) and 4-vinyl pyridine (4-VP). In this study, we hoped to find a kind of monomer which could not only be as functional monomer but also as fluorescent monomer and it was just an attempt. Fluorescein as a common organic dye has been widely applied into fluorescence detection. It was well-known that there was no double bond in fluorescein for coupling with other composition. Therefore, ally fluorescein was synthesized via leading in double bond. Chemical structure and synthetic scheme of ally fluorescein were shown in Figs. S1 and S2, respectively. Fluorescent dye (ally fluorescein) was chosen as functional monomer replacing traditional functional monomer because ally fluorescein and BC both had regular benzene ring, which could form accumulation of benzene ring and generate acting force between ally fluorescein and BC. As shown in Fig. 1, conjugate action produced through phenyl group of ally fluorescein and BC made them connect closely, then double bond of ally fluorescein reacted with double bond of TRIM and generate the polymer layer.

In this study, our purpose of research was to find a new rapid and effective method to achieve the selective recognition of BC with minimum non-specific binding. Therefore, fluorescent molecularly imprinted polymers (SiO₂-MPTMS@FMIPs) were synthesized via precipitation polymerization. The Schematic illustration for the preparation of SiO₂-MPTMS@FMIPs was displayed in Fig. 1. FMIPs were obtained using beta-cyfluthrin as target molecule, ally fluorescein as functional monomer, trimethylolpropane trimethacrylate (TRIM) as crosslinker, azobisisobutyronitrile (AIBN) as initiator and acetonitrile as solvent, respectively. The synthesis method of FNIPs was the same as FMIPs without BC template. The characterization of SiO₂-MPTMS@FMIPs and SiO₂-MPTMS@FNIPs was observed via FTIR, SEM, TEM, LSCM and TGA. Moreover, fluorescence intensity was measured via a fluorescence spectrophotometer. The selective recognition of target molecules of FMIPs was illustrated by the different fluorescent intensity of BC with the other pyrethroid pesticides. In this study, we chose the three washing water from that local vegetables because people's health may be threatened via eating those vegetables which content of pyrethroid pesticides was out of limit. On the whole, through application to water sample analysis in agricultural products, it can be found that SiO₂-MPTMS@FMIPs has a broad prospect in agricultural products.

2. Experimental procedures

2.1. Reagents and chemicals

Tetraethyl orthosilicate (TEOS, ≥99.0%, GC), ammonium hydroxide (25.0%–28.0%, AR), 3-(methacryloyloxy) propyltrimethoxysilane

Table 1
Different methods of detection Beta-Cyfluthrin.

Methodology	Detection method	Limit of detection (LOD)	Advantages	Disadvantages	Reference
This method	FMIPs	10.11 nM L ⁻¹	High sensitivity, simplicity, efficiency, speed, low LOD	Immaturity, boundedness	–
Galera et al.	HPLC	0.013–0.049 μg mL ⁻¹	Accuracy, great stability, low LOD	Multistep, time-consuming, high cost	Ge et al. (2011)
Ferreira et al.	LC-MSPD	0.02–0.03 μg g ⁻¹	High recoveries, low LOD	Multistep, time-consuming, high cost	Griesinger et al. (2014)
Ma and Chen	MMIPs	0.0072 mg kg ⁻¹	Simplicity, sensitivity and reliability, low LOD	Multistep, inaccuracy	Lv et al. (2013)
Shi et al.	GC-MISPE	16.6–37.0 ng L ⁻¹	Accuracy, the excellent group-selective enrichment, low LOD	Multistep, immaturity, boundedness	Ma and Chen (2014)

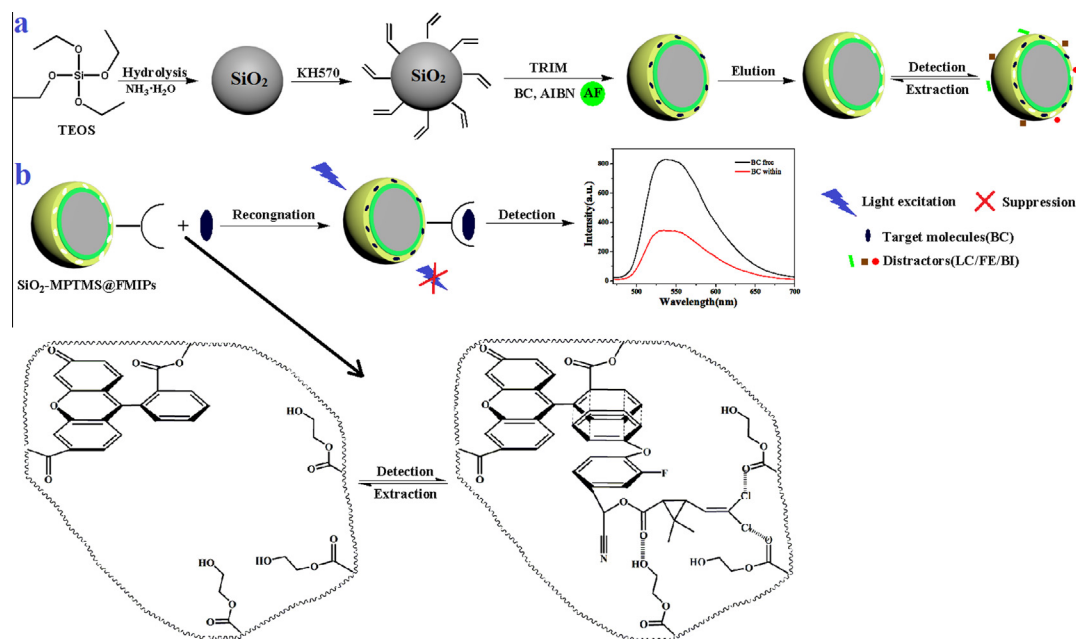


Fig. 1. Schematic illustration for the preparation of SiO₂-MPTMS@FMIPs.

(MPTMS, $\geq 97.0\%$), trimethylolpropane trimethacrylate (TRIM, 80.0%), were all purchased from Aladdin Chemistry Co. Ltd. (Shanghai, China). Acetonitrile ($\geq 99.0\%$), ethyl alcohol ($\geq 99.7\%$), fluorescein (AR), allyl bromide (CP), hydroquinone (AR), iodine (AR), *N,N*-Dimethylformamide (DMF, $\geq 99.5\%$, AR), potassium carbonate (K₂CO₃, AR), trichloromethane ($\geq 99.0\%$, AR), silica gel, methyl alcohol ($\geq 99.5\%$), acetic acid ($\geq 99.5\%$) were all purchased from Sinopharm Chemical Reagent Co., Ltd. (Shanghai, China). 2,2'-Azo bis(isobutyronitrile) (AIBN, AR) was obtained from Tianjin Guangfu Fine Chemical Research Institute (Tianjin, China). All the pyrethroid pesticides, including beta-cyfluthrin (BC), λ -Cyhalothrin (LC), esfenvalerate (FE) and bifenthrin (BI) were obtained from Ying-tianyi standard sample company (Beijing, China). Doubly distilled water was used for cleaning processes. The chemical structures of crosslinker, template, and related compounds were shown in Fig. S1.

2.2. Instruments

Infrared spectra (4000–400 cm⁻¹) was measured on a Nicolet NEXUS-470 FT-IR apparatus which was produced from USA. The morphologies and sizes of SiO₂-MPTMS@FMIPs/SiO₂-MPTMS@FNIPs were observed via a scanning electron microscope (SEM, JEOL, JSM-7001F) and a transmission electron microscope (TEM, JEOL, JEM-2100). Fluorescence intensity was recorded by Cary Eclipse fluorescence spectrophotometer (Varian, USA). Laser confocal microscopy images of the samples were observed using a TCS SP5 II confocal microscope (Leica, Germany) with a 488 nm excitation light source. Transient fluorescence spectra were determined on Quanta Master™ 40 Spectrofluorometer (Photon Technology International, U.S.A.). TGA of the samples was performed for powder samples (about 10 mg) using a Diamond TG/DTA instruments (Perkin-Elmer, U.S.A.) under a nitrogen atmosphere up to 800 °C with a heating rate of 10 °C·min⁻¹.

2.3. Synthesis of allyl fluorescein

Liu and co-workers have successfully synthesized allyl fluorescein with a simple and convenient method (Liu et al., 2009). In addition, synthesizing process of the allyl fluorescein was shown

in Fig. S2. The mixture of fluorescein (2.00 g, 6.0 mmol), allyl bromide (2.42 g, 20.0 mmol), K₂CO₃ (4.97 g, 36.0 mmol), hydroquinone and iodine (trace) were added to dry DMF (60 ml) in the dark under a nitrogen atmosphere for 25 h at 71 °C. The solvent was removed under reduced pressure. Then, the pure product was obtained via column chromatographic in which trichloromethane was used as eluent (yield, 63%).

2.4. Synthesis of SiO₂ and SiO₂-MPTMS

SiO₂, which has an excellent chemical stability and a characteristic of facile modification, has widely been utilized in basis material, especially in the field of nanometer materials (Li, Cui, Li, & Li, 2011). In this scheme, SiO₂ was obtained via an emulsion polymerization. A mixture of distilled water (28 mL), ethyl alcohol (65 mL), ammonium hydroxide (7 mL), TEOS (1 mL) were stirred at room temperature for 0.5 h. SiO₂ (200 mg) obtained from above process was dispersed in 60 mL ethanol by sonication for 1 h, followed by the addition of 2 mL MPTMS for 24 h at 40 °C and SiO₂-MPTMS was separated with solvent by centrifuge and repeatedly washed by ethanol alcohol.

2.5. Synthesis of SiO₂-MPTMS@FMIPs and SiO₂-MPTMS@FNIPs

SiO₂-MPTMS@FMIPs and SiO₂-MPTMS@FNIPs were both synthesized via precipitation polymerization according to the following procedure. Briefly, a mixture of beta-cyfluthrin (250 mg) as the template, TRIM (0.40 mL) as the cross-linking agent, Allyl fluorescein (500 mg) as functional monomer were added into a stand-up flask which has 60 ml of acetonitrile as a solvent of system with a magnetic stirring for prepolymerization for 24 h at room temperature. SiO₂-MPTMS (300 mg) was dispersed in acetonitrile (60 mL) with ultrasonic concussion for 2 h. Then, 50 mg of AIBN were added into the reaction mixture under a nitrogen atmosphere for 30 min and sealed. The flask was allowed to proceed for 48 h at 60 °C. The product obtained from the above steps was separated with solvent via the centrifuge and repeatedly washed by ethanol alcohol (yield: 65.4%).

Refer to the steps above, SiO₂-MPTMS@FNIPs was prepared except that template was omitted (yield: 63.7%).

3. Results and discussion

3.1. Characterization of SiO₂-MPTMS@FMIPs and SiO₂-MPTMS@FNIPs

Analysis of FTIR spectroscopy is a kind of general analysis method to check whether the synthesis is successful or not. The FTIR spectrum of SiO₂, SiO₂-MPTMS@FMIPs removed target molecule and SiO₂-MPTMS@FNIPs could be measured in Fig. S3. The strong and broad peak at 1103 cm⁻¹ indicated asymmetric stretching of Si–O–Si. The peaks at 473 cm⁻¹ and 803 cm⁻¹ represented Si–O asymmetric stretching vibration and bending vibration. These discussions adequately suggested that SiO₂ microspheres were successfully prepared via emulsion polymerization. Compared with the FTIR spectrum of SiO₂, SiO₂-MPTMS@FMIPs prepared by precipitation polymerization not only had the characteristic peaks at 1103, 803, 473 cm⁻¹ but also had other asymmetric stretching vibration and bending vibration. The peak of the aliphatic C–H stretching was indicated at 2977 cm⁻¹. The peaks of C=O and C–H of phenyl group arose at 1736 cm⁻¹. The broad peak shown at 1600 cm⁻¹ suggested existence of the group of –COO–. The peak of 1651 cm⁻¹ belonged to some unreacted C=C double bonds of TRIM used as cross-linker. Moreover, the peak of –CH₂– was observed at 1471 cm⁻¹ and the peak at 1388 cm⁻¹ represented the flexural vibration of –CH₃. As to the above-mentioned analysis, the MIPs lays including allyl fluorescein and TRIM had been successfully bundled on the surface of SiO₂. Certainly, FTIR spectrum of SiO₂-MPTMS@FNIPs was similar to SiO₂-MPTMS@FMIPs.

To observably show that FMIPs has been successfully synthesized with BC, the Energy Dispersive Spectrometer (EDS) of SiO₂-MPTMS@FMIPs was measured and the EDS spectrum was shown in Fig. S4. EDS spectrum showed peaks of six elements including C, O, F, Cl, Si, Au. It was found that F and Cl elements only existed in BC and the reason which it contained Au element was that the samples must be plated a layer of gold. The peaks of F and Cl elements illustrated that SiO₂-MPTMS@FMIPs with BC had been prepared successfully. Moreover, we found that content of Si element was far more than C, O, F, Cl. In another word, the core-shell structure had a thin shell.

As shown in Fig. S5, the size and dispersibility of SiO₂, SiO₂-MPTMS@FMIPs and SiO₂-MPTMS@FNIPs were observed by SEM and TEM techniques. The SEM and TEM images of SiO₂ were observed in Fig. S5a,d. It not only shown the diameter of SiO₂ was about 200 nm but also SiO₂ microspheres with smooth surface had a good dispersibility. The images of SiO₂-MPTMS@FMIPs were shown in Fig. S5b,e. It was seen that the molecularly imprinted microspheres had regular spherical morphology with a good dispersibility. Moreover, an average diameter of FMIPs with a relative uniformity was approximately about 300 nm. That is to say, imprinted layer was almost approximately 50 nm. The SEM and TEM images of SiO₂-MPTMS@FNIPs shown in Fig. S5c,f were distinctly observed and the smoothness and regulation were worse compared with the FMIPs. The average size of FNIPs and imprinted layer were similar with FMIPs. In brief, it demonstrated that microspheres of SiO₂-MPTMS@FMIPs and SiO₂-MPTMS@FNIPs have been successfully prepared and the molecularly imprinted microspheres synthesized have attained the nanometer scale which can more precisely recognize the target molecule.

In order to observed the fluorescence characteristic and dispersibility in the ethyl alcohol rapidly and efficiently, the fluorescent images of SiO₂-MPTMS@FMIPs and SiO₂-MPTMS@FNIPs were measured via laser scanning confocal microscope (LSCM). First, excitation wavelength and emission wavelength of Allyl fluorescein measured were 488 nm and 525 nm, respectively. Fluorescence characteristic of MIPs and NIPs was shown in Fig. S6a,b, fluorescent dye was added to MIPs and NIPs via succinct and

precise precipitation polymerization. Besides, the polymers of SiO₂-MPTMS@FMIPs and SiO₂-MPTMS@FNIPs both had excellent dispersity. In short, FMIPs and FNIPs based on both molecularly imprinted technology and the fluorescence detection were prepared with excellent dispersity.

The curves of SiO₂, SiO₂-MPTMS@FMIPs and SiO₂-MPTMS@FNIPs were shown via TGA technique at a heating rate of 10 °C·min⁻¹ from room temperature to 800 °C under N₂ atmosphere. As shown in Fig. S7, the weight losses of SiO₂ were about 12.33%. The reason for the weight losses of SiO₂ was only the absence of water. TGA curves of SiO₂ trended to a parallel and did not decline any more after reaching 800 °C, which illustrated SiO₂ was stable before 800 °C. The weight losses of SiO₂-MPTMS@FMIPs and SiO₂-MPTMS@FNIPs before 800 °C were ~56.5% and ~54.06%, respectively. However, in theory, the weight losses of FMIPs and FNIPs with the same element and equivalent substance are homologous due to the difference of crystal water and water in the test environment. The whole process of thermo weightless was divided roughly into two stages. At the beginning, the weight losses of FMIPs and FNIPs before 270 °C were 6.87% and 9.22%, respectively. The phenomenon might be attributed to crystal water or water absorbed in atmosphere in different degrees. In addition, the curves of FMIPs and FNIPs started to decline at 300 °C and 350 °C, respectively. The weight losses of imprinted layer were 49.68% and 44.84%. And the both end temperature was 480 °C. In other words, polymers had an excellent thermostability. These discussions illustrated that the polymers including FMIPs and FNIPs had been grafted onto the surface of SiO₂ with an excellent thermostability.

3.2. Fluorescence detection of SiO₂-MPTMS@FMIPs

The fluorescence intensity of MIPs and NIPs with the excitation wavelength of 488 nm was monitored at room temperature. The SiO₂-MPTMS@FMIPs (50 mg) was dispersed in 100 mL volumetric flask with ethyl alcohol solution, which was prepared for fluorescence detection. Immediately following that, 5.0 mL of BC solution of different concentration (0–1.5 μM) prepared was added into colorimetric cylinder with 5.0 mL sample solution, respectively. The mixture was dispersed with ultrasonic concussion for 5 min so that target molecule could adequately combine with FMIPs. The linear relationship of the fluorescence quenching efficiency of the SiO₂-MPTMS@FMIPs with BC was described by (F₀/F–1) versus the concentration (nM) in Fig. 3. The homologous procedure was performed for the SiO₂-MPTMS@FNIPs.

As shown in Fig. 2, it was obviously that with the increasing of concentration of BC, fluorescence intensity of both SiO₂-MPTMS@FMIPs and SiO₂-MPTMS@FNIPs gradually decreased. Moreover, the downtrend of fluorescence intensity curves of SiO₂-MPTMS@FMIPs was more obvious compared with SiO₂-MPTMS@FNIPs. Therefore, the detection capacity of FMIPs with BC was more excellent than FNIPs. In other words, BC molecules could be efficiently detected via fluorescence quenching. The selectivity and sensitivity of nanocomposite were evaluated via the fluorescence intensity curves which illustrated the spatial adsorption sites could be incorporated into SiO₂-MPTMS@FMIP matrix. In the end, we could summarize the above phenomenon mirrored in the fluorescence intensity curves confirmed SiO₂-MPTMS@FMIPs had been prepared successfully and had a detection of BC.

To investigate thoroughly the fluorescence quenching mechanism of SiO₂-MPTMS@FMIPs with BC, the quenching efficiency of FMIPs microspheres was evaluated by the Stern–Volmer equation, as follow:

$$F_0/F = 1 + K_{sv}[Q] \quad (1)$$

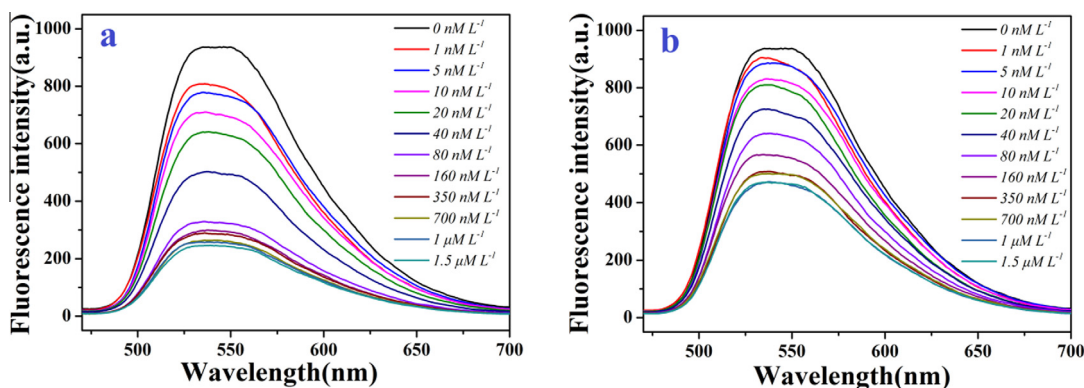


Fig. 2. Fluorescence intensity curves of SiO₂-MPTMS@FMIPs (a) and SiO₂-MPTMS@FNIPs (b).

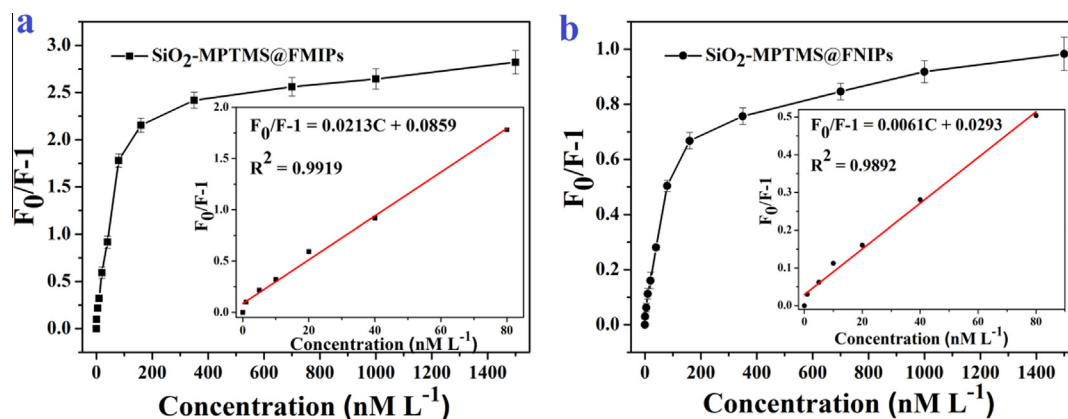


Fig. 3. Fluorescence quenching efficiency changed according to BC concentration. (Insets) Linear equations of SiO₂-MPTMS@FMIPs (a) and SiO₂-MPTMS@FNIPs (b).

where F_0 is the initial fluorescence intensity before quencher (BC) is added. F is the fluorescence intensity in the presence of quencher, $[Q]$ is concentration of the quencher and K_{SV} ($L \text{ mol}^{-1}$) is quenching constant with BC.

The reproducibility experiments were repeated five times with a uniform method of FMIPs. The data obtained by reproducibility experiments was shown in Fig. 3. The good linear relationship with fluorescence intensity appeared in the concentration range of 0–80 nM. Moreover, the linear equation of SiO₂-MPTMS@FMIPs was $F_0/F-1 = 0.0213C + 0.0859$, where the corresponding correlation coefficient was $R^2 = 0.9919$ and $K_{SV(\text{FMIPs})} = 0.0213E6 \text{ L mol}^{-1}$. The limit of detection is evaluated with the equation $\text{LOD} = 3\sigma/S$ and is found to be 10.11 nM, where σ is the standard deviation of the blank signal and S is the slope of the linear calibration plot. In addition, Fig. 3b showed the linear relationship of SiO₂-MPTMS@FNIPs. The linear equation was $F_0/F-1 = 0.0061C + 0.0293$ in the concentration range of 10.11–80 nM with a good linear relationship, where the corresponding correlation coefficient was 0.9892 and $K_{SV(\text{FNIPs})} = 0.0061E6 \text{ L mol}^{-1}$. However, as shown in Fig. 3a,b, the fluorescence quenching curves of both FMIPs and FNIPs became gentle gradually when concentration of quencher surpassed 80 nM, and it remain gentle till saturation.

The quenching process of SiO₂-MPTMS@FMIPs with quencher may be dynamic quenching, which the quenching process occurs in interactions with excited state molecules of quencher and FMIPs. In other words, excited state molecules of quencher and FMIPs crash each other directly or occurs in optical collision, which make fluorescence intensity of FMIPs decay. Therefore, Steady-state and time-resolved fluorescence measurements were performed to elucidate the fluorescence quenching of FMIPs

(Marmé, Knemeyer, Sauer, & Wolfrum, 2003), concrete analysis as follow;

The transient fluorescence curves of SiO₂-MPTMS@FMIPs and SiO₂-MPTMS@FNIPs were shown in Fig. S8. The linear relation of the fluorescence intensity (F) and time (t) was evaluated via an exponential function, as follow:

$$F(t) = A \exp(-t/\tau) \quad (2)$$

where τ represents the lifetime and A represents the amplitude.

As shown in Fig. S8, the curves of SiO₂-MPTMS@FMIPs and SiO₂-MPTMS@FNIPs both had obvious trend of rising and decaying between 130 and 135 ns. The decay equation of SiO₂-MPTMS@FMIPs was $F(t) = 4.799E30 \exp(-t/2.072) + 8.112$ and the corresponding correlation coefficients (R^2) was $R^2 = 0.9687$ via Eq. (2). Moreover, the lifetime of SiO₂-MPTMS@FMIPs could be obtained via Eq. (2) and the value was 2.072 ns. Homoplastically, the decay equation of SiO₂-MPTMS@FNIPs was $F(t) = 6.846E27 \exp(-t/2.318) + 9.238$ with $R^2 = 0.9360$ via Eq. (2) and the lifetime was 2.318 ns.

According to the difference that whether the lifetime with the quenching agent or not, the Eq. (1) was modified to another form, as follow:

$$\tau_0/\tau = 1 + K_q\tau_0[Q] \quad (3)$$

where τ_0 is the lifetime without the quenching agent, τ is the lifetime with the quenching agent and K_q is the rate constant of bimolecular quenching process.

Comparing Eq. (1) with Eq. (3), it suggested amazingly that $K_{SV} = K_q\tau_0$. The above analysis of SiO₂-MPTMS@FMIPs indicated that $K_{SV(\text{FMIPs})} = 0.0213E6 \text{ L mol}^{-1}$, $\tau_0 = 2.072 \text{ ns}$. Then, K_q was

calculated, and $K_{q(\text{FMIPs})} = 1.028\text{E}10 \text{ L mol}^{-1} \text{ s}^{-1}$. The similar calculative process of $\text{SiO}_2\text{-MPTMS@FNIPs}$ was performed tautologically, in which $K_{q(\text{FNIPs})} = 2.632\text{E}9 \text{ L mol}^{-1} \text{ s}^{-1}$. As shown in Eq. (3), the rate constant of bimolecular quenching process (K_q) represented bimolecular encountering frequency orders of magnitude. The rate constant of bimolecular quenching process (K_q) was about $1.0\text{E}9 \sim 2.0\text{E}10 \text{ L mol}^{-1} \text{ s}^{-1}$ for the dynamic quenching due to the various balanced result (Ware, 1962). The above discussion illustrated $K_{q(\text{FMIPs})} = 1.028\text{E}10 \text{ L mol}^{-1} \text{ s}^{-1}$ and $K_{q(\text{FNIPs})} = 2.632\text{E}9 \text{ L mol}^{-1} \text{ s}^{-1}$ were both in the range. Therefore, the fluorescence quenching of $\text{SiO}_2\text{-MPTMS@FMIPs}$ and $\text{SiO}_2\text{-MPTMS@FNIPs}$ is dynamic quenching. Comparing $K_{q(\text{FMIPs})}$ with $K_{q(\text{FNIPs})}$, it was found that $K_{q(\text{FMIPs})} > K_{q(\text{FNIPs})}$ owing to the existence of many specific binding sites in $\text{SiO}_2\text{-MPTMS@FMIPs}$ which increased the specific surface area and acting force between $\text{SiO}_2\text{-MPTMS@FMIPs}$ and target molecule. FMIPs was more likely to occur with bimolecular dynamic collision. In another word, that was the reason why the quenching phenomenon of FMIPs was more obvious than that of FNIPs. The above analysis demonstrated FMIPs had not only a high quenching rate but also a precise detection range for BC.

3.3. Selectivity determination of $\text{SiO}_2\text{-MPTMS@FMIPs}$ and $\text{SiO}_2\text{-MPTMS@FNIPs}$

In this study, our main aim is to investigate the selectivity determination of $\text{SiO}_2\text{-MPTMS@FMIPs}$. Therefore, several pyrethroids with the possibility of potential interference including LC, BI, FE and the bend solutions with BC were selected to compare with BC. The $\text{SiO}_2\text{-MPTMS@FMIPs}$ (50 mg) were dispersed in 10 mL of ethanol solutions with 40 nM of LC, FE, BI and BC, respectively. The mixtures were vibrated with ultrasonic for 5 min to adequately combine target molecule with FMIPs.

As shown in Fig. 4a, fluorescence intensity curves of $\text{SiO}_2\text{-MPTMS@FMIPs}$ for BC and the mixture including BC were much lower than that of the structural analogues. In other words, obviously, the absorption capacity of $\text{SiO}_2\text{-MPTMS@FMIPs}$ for BC was superior to other several pyrethroids. Moreover, it was amazing to find that fluorescence intensity curve of FMIPs with BC was slightly lower than that of mixture but the distinction was not obvious. The above analysis confirmed that the selectivity determination of $\text{SiO}_2\text{-MPTMS@FMIPs}$ with BC was not influenced by interference of competitors.

Quenching efficiency of $\text{SiO}_2\text{-MPTMS@FMIPs}$ and $\text{SiO}_2\text{-MPTMS@FNIPs}$ by different kinds of 40 nM pyrethroids was shown in Fig. S9. Obviously, quenching efficiency of $\text{SiO}_2\text{-MPTMS@FMIPs}$ with BC was superior to that of other structural analogues and $\text{SiO}_2\text{-MPTMS@FNIPs}$. Moreover, quenching efficiency of $\text{SiO}_2\text{-MPTMS@FNIPs}$ with four kinds of pyrethroids was almost

not alternative, which illustrated $\text{SiO}_2\text{-MPTMS@FNIPs}$ had worse selectivity determination with pyrethroids.

To sum up, $\text{SiO}_2\text{-MPTMS@FMIPs}$ had a good selectivity for BC without interference of other pyrethroids and it is also confirmed that the $\text{SiO}_2\text{-MPTMS@FMIPs}$ microspheres had been prepared successfully.

3.4. The regeneration experiments of $\text{SiO}_2\text{-MPTMS@FMIPs}$

The stability and cyclic experiments of $\text{SiO}_2\text{-MPTMS@FMIPs}$ were investigated via measuring the fluorescence intensity of $\text{SiO}_2\text{-MPTMS@FMIPs}$ with BC and used repeatedly for eight times. In belief, $\text{SiO}_2\text{-MPTMS@FMIPs}$ (100 mg) were dispersed in 40 nM BC solutions and vibrated for 5 min before fluorescence measurement. After the measurement, $\text{SiO}_2\text{-MPTMS@FMIPs}$ were washed with methanol-acetic acid solution (9:1, v/v) to separate targets. The above process was repeated eight times with an identical batch of $\text{SiO}_2\text{-MPTMS@FMIPs}$. The fluorescence intensity histogram was presented in Fig. S10. The fluorescence intensity after five cyclic experiments just declined a little so that $\text{SiO}_2\text{-MPTMS@FMIPs}$ can be reused at least five times with a good selectivity determination.

3.5. Application to water sample analysis

In this study, to evaluate the applicability of $\text{SiO}_2\text{-MPTMS@FMIPs}$ in four times, we chose distilled water and the same vegetable washing water which was extracted from three local vegetable farms and marked as wash water 1, 2, 3. Specific experimental procedure as follow; we chose the same vegetables came from three local vegetable farms and these vegetables were immersed into the distilled water over night. Then, these water was extracted via centrifuge. In an addition, 100 mg of $\text{SiO}_2\text{-MPTMS@FMIPs}$ were added into 100 mL of 40 nM BC solution and vibrated for 5 min before fluorescence measurement. The same experiment was repeated five times, respectively. The content of BC found can be calculated via the equation ($F_0/F-1 = 0.0213C + 0.0859$). Results of BC found and Recovery was given as the mean \pm SD of the data ($n = x$) in Table 2.

As shown in Table 2, the recovery of distilled water was lower than 100% but it was close to 100%. Therefore, it demonstrated that it was quite precise in the concentration range of 10.11–80 nM. However, all the recovery of wash water 1, 2, 3 was larger than 100% which illustrated the there was a certain amount of BC in sample water. It was investigated that pyrethroids were as main pesticide in the locality. Moreover, it was found that fluctuation value of recovery was low and the recovery value of three tests in the same water sample was approach. Therefore, the precision

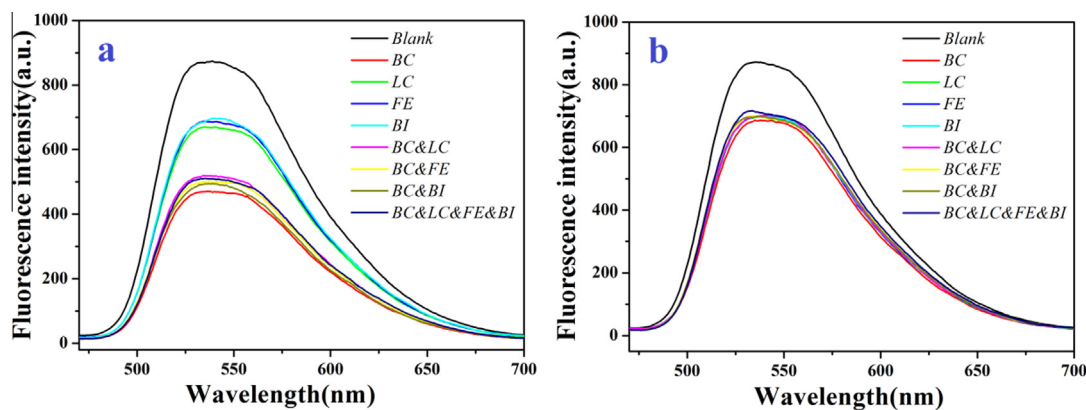


Fig. 4. Fluorescence intensity curves of $\text{SiO}_2\text{-MPTMS@FMIPs}$ (a) and $\text{SiO}_2\text{-MPTMS@FNIPs}$ (b) by different kinds of 40 nM pyrethroids.

Table 2
Recovery of BC in water samples at different concentration levels.

Samples	Test Number	BC Added (nM)	BC Found (nM)	Recovery (%)
Distilled water	1	2	1.982 ± 0.028	99.1 ± 1.40
	2	4	3.964 ± 0.054	99.1 ± 1.35
	3	8	7.892 ± 0.103	98.7 ± 1.29
Wash water 1	1	2	2.182 ± 0.026	109.1 ± 1.30
	2	4	4.400 ± 0.051	110.0 ± 1.28
	3	8	8.942 ± 0.112	111.8 ± 1.40
Wash water 2	1	2	2.142 ± 0.024	107.1 ± 1.20
	2	4	4.240 ± 0.052	106.5 ± 1.30
	3	8	8.568 ± 0.108	107.1 ± 1.35
Wash water 3	1	2	2.094 ± 0.022	104.7 ± 1.10
	2	4	4.160 ± 0.048	104.0 ± 1.20
	3	8	8.308 ± 0.107	103.8 ± 1.34

Table 3
Recovery of BC in water samples at different concentration levels by using GC and HPLC.

Samples	Test Number	BC Added (nM)	GC		HPLC	
			BC Found (nM)	Recovery (%)	BC Found (nM)	Recovery (%)
Distilled water	1	2	1.926 ± 0.043	96.3 ± 2.15	1.946 ± 0.048	97.3 ± 2.40
	2	4	3.845 ± 0.063	96.1 ± 1.58	3.904 ± 0.087	97.1 ± 2.18
	3	8	7.724 ± 0.188	96.6 ± 2.35	7.835 ± 0.206	97.9 ± 2.56
Wash water 1	1	2	2.138 ± 0.049	106.9 ± 2.45	2.152 ± 0.047	107.6 ± 2.35
	2	4	4.300 ± 0.082	107.5 ± 2.05	4.248 ± 0.078	106.2 ± 1.95
	3	8	8.864 ± 0.128	110.8 ± 1.60	8.696 ± 0.192	108.7 ± 2.40
Wash water 2	1	2	2.136 ± 0.038	106.8 ± 1.90	2.110 ± 0.045	105.5 ± 2.25
	2	4	4.248 ± 0.085	106.2 ± 2.12	4.256 ± 0.089	106.4 ± 2.23
	3	8	8.456 ± 0.178	105.7 ± 2.23	8.400 ± 0.210	105.0 ± 2.63
Wash water 3	1	2	2.082 ± 0.037	104.1 ± 1.85	2.064 ± 0.043	103.2 ± 2.15
	2	4	4.160 ± 0.124	103.6 ± 3.10	4.084 ± 0.088	102.1 ± 2.20
	3	8	8.216 ± 0.126	102.7 ± 1.58	8.088 ± 0.187	101.1 ± 2.34

was high. In addition, the recovery of wash water 1 was much higher than others and the recovery of wash water 3 was quite low. Therefore, the dosage of BC pesticide of farm 1 was higher and we must repeatedly wash the vegetables in farm 1. On the whole, SiO₂-MPTMS@FMIPs can be applied to real samples.

To protrude the superiority of this experimental method in water sample analysis, we have done the contrast experiment by using GC and HPLC, respectively. The data of GC and HPLC was shown in Table 3. Obviously, it was seen that in Table 3, the recovery of BC found of distilled water was both lower than this experimental method. In theory, the data was close to 100%, because no BC was added and no BC existed in distilled water. Therefore, it was illustrated that precision of this experimental method in sample water was approach to GC and HPLC. Of cause, we can see that the recovery fluctuation value of GC and HPLC was even bigger than this method and it demonstrated that it has higher detection stability than GC and HPLC. On the whole, the precision and detection stability was excellent in sample water.

4. Conclusion

In summary, we can combine surface imprinting technique with fluorescent detection technique to synthesize the core-shell SiO₂-MPTMS@FMIPs binding on the surface of SiO₂, which can be used in the selective detection of BC. The characterization of the synthesized microspheres of spherical shape was investigated in detail, which included in morphology, thermal gravity analysis, molecular recognition, regeneration and fluorescence detection of target molecule. Core-shell microspheres had excellent dispersity and thermostability. The fluorescence intensity curves of BC were detected via the Stern-Volmer equation with the fluorescence spec-

trophotometer, which illustrated fluorescence property and found the limit of detection was 10.11 nM. Quenching efficiency of SiO₂-MPTMS@FMIPs confirmed that good selectivity determination for BC was measured in the mixed solutions of the structurally analogous. The good reproducibility of SiO₂-MPTMS@FMIPs was reflected via regeneration experiment. On the whole, the paper not only provide a new fluorescent molecularly imprinted technology without functional monomer for recognizing nonfluorescent pyrethroid pesticides but also improved the potential application of molecularly imprinted polymers.

Acknowledgements

This work was financially supported by the National Natural Science Foundation of China (No. 21277063, No. 21407057, No. U1407123, No. 21507045, and No. 21576111), Natural Science Foundation of Jiangsu Province (No. BK20140535, No. BK20140580), National Postdoctoral Science Foundation (No. 2013M540423, No. 1401108C, No. 2014M561595 and No. 2015M581744). Research Fund for the Doctoral Program of Higher Education of China (No. 20133227110010).

Appendix A. Supplementary data

Detailed experimental characterization for polymers such as the fluorescent equation, measurements, and additional figures (FT-IR, SEM, TEM, LCSM images, thermal gravity analysis (TGA), results of competitive and regenerative experiments).

Supplementary data associated with this article can be found, in the online version, at <http://dx.doi.org/10.1016/j.foodchem.2016.09.028>.

References

- Alexander, C., Andersson, H. S., Andersson, L. I., Ansell, R. J., Kirsch, N., Nicholls, I. A., et al. (2003). Molecular imprinting science and technology: A survey of the literature for the years up to and including 2003. *Journal of Molecular Recognition*, 19, 106–180.
- Andersson, L. I. (2000). Molecular imprinting: Developments and applications in the analytical chemistry field. *Journal of Chromatography B*, 745, 3–13.
- Caro, E. R., Marce', M., Borrull, F., Cormack, P. A. G., & Sherrington, D. C. (2006). Application of molecularly imprinted polymers to solid-phase extraction of compounds from environmental and biological samples. *TrAc Trends in Analytical Chemistry*, 25(2), 143–154.
- Chalányová, M., Paulechová, M., & Hutta, M. (2006). Method of analysis of a selected group of pyrethroids in soil samples using off-line flow-through extraction and on-column direct large-volume injection in reversed phase high performance liquid chromatography. *Journal of Separation Science*, 29, 2149.
- Chen, L. X., Xu, S. F., & Li, J. H. (2011). Recent advances in molecular imprinting technology: Current status, challenges and highlighted applications. *Chemical Society Reviews*, 40, 2922–2942.
- Cimpou, C., Hosu, A., & Hodisan, S. (2006). Analysis of some steroids by thin-layer chromatography using optimum mobile phases. *Journal of Pharmaceutical and Biomedical Analysis*, 41, 633–637.
- Dalluge, J., Beens, J., & Brinkman, U. A. T. (2003). Comprehensive two-dimensional gas chromatography: A powerful and versatile analytical tool. *Journal of Chromatography A*, 1000, 69–108.
- European Commission. (2002). Health and Consumer Protection Directorate-General (Beta-cyfluthrin), Appendix I.
- Ferreira, J. A., Santos, L. F. S., Souza, N. R. S., Navickiene, S., Oliveira, F. A., & Talamini, V. (2013). MSPD sample preparation approach for reversed-phase liquid chromatographic analysis of pesticide residues in stem of coconut palm. *Bulletin of Environmental Contamination and Toxicology*, 91, 160–164.
- Galera, M. M., Garcia, M. D. G., & Valverde, R. S. (2006). Determination of nine pyrethroid insecticides by high-performance liquid chromatography with post-column photoderivatization and detection based on acetonitrile chemiluminescence. *Journal of Chromatography A*, 1113, 191–197.
- Gao, L., Li, X. Y., Zhang, Q., Dai, J. D., Wei, X., Song, Z. L., et al. (2014). Molecularly imprinted polymer microspheres for optical measurement of ultra trace nonfluorescent cyhalothrin in honey. *Food Chemistry*, 156, 1–6.
- Ge, S. G., Lu, J. J., Ge, L., Yan, M., & Yu, J. H. (2011). Development of a novel deltamethrin sensor based on molecularly imprinted silica nanospheres embedded CdTe quantum dots. *Spectrochimica Acta Part A: Molecular and Biomolecular Spectroscopy*, 79, 1704–1709.
- Griesinger, H., Fuchs, B., Süß, R., Matheis, K., Schulz, M., & Schiller, J. (2014). Stationary phase thickness determines the quality of thin-layer chromatography/matrix-assisted laser desorption and ionization mass spectra of lipids. *Analytical Biochemistry*, 451, 45–47.
- Hamscher, G., Sczesny, S., Hoper, H., & Nau, H. (2002). Determination of persistent tetracycline residues in soil fertilized with liquid manure by high-performance liquid chromatography with electrospray ionization tandem mass spectrometry. *Analytical Chemistry*, 74, 1509–1518.
- Haupt, K., & Mosbach, K. (2000). Molecularly imprinted polymers and their use in biomimetic sensors. *Chemical Reviews*, 100, 2495–2504.
- He, C. Y., Long, Y. Y., Pan, J. L., Li, K. A., & Liu, F. (2007). Application of molecularly imprinted polymers to solid-phase extraction of analytes from real samples. *Journal of Biochemical and Biophysical Methods*, 70, 133–150.
- Holmstead, R. L., & Fullmer, D. G. (1977). Photodecarboxylation of cyanohydrin esters. Models for pyrethroid photodecomposition. *Journal of Agricultural and Food Chemistry*, 25, 56.
- Jing, T., Du, H. R., Dai, Q., Xia, H., Niu, J. W., Hao, Q. L., et al. (2010). Magnetic molecularly imprinted nanoparticles for recognition of lysozyme. *Biosensors & Bioelectronics*, 26, 301–306.
- Katagi, T. (1991). Photodegradation of the pyrethroid insecticide esfenvalerate on soil, clay minerals, and humic acid surfaces. *Journal of Agricultural and Food Chemistry*, 39, 1351–1356.
- Katagi, T. (1993). Photodegradation of esfenvalerate in clay suspensions. *Journal of Agricultural and Food Chemistry*, 47, 2178–2183.
- Lakowicz, J. R. (2005). Radiative decay engineering 5: Metal-enhanced fluorescence and plasmon emission. *Analytical Biochemistry*, 337, 171–194.
- Lehotay, S. J., Lightfield, A. R., Harman-Fetcho, J. A., & Donoghue, D. J. (2001). Analysis of pesticide residues in eggs by direct sample introduction/gas chromatography/tandem mass spectrometry. *Journal of Agricultural and Food Chemistry*, 49, 4589–4596.
- Li, Y. L., Cui, Z. M., Li, D. P., & Li, H. B. (2011). Colorimetric determination of pyrethroids based on core-shell Ag@SiO₂ nanoparticles. *Sensors and Actuators B: Chemical*, 155(2), 878–883.
- Li, X., & Husson, S. M. (2006). Adsorption of dansylated amino acids on molecularly imprinted surfaces: A surface plasmon resonance study. *Biosensors & Bioelectronics*, 22, 336–348.
- Liu, Q. H., Liu, J., Guo, J. C., Yan, X. L., Wang, D. H., Chen, L., et al. (2009). Preparation of polystyrene fluorescent microspheres based on some fluorescent labels. *Journal of Materials Chemistry*, 19, 2018–2025.
- Lv, Y. Q., Lin, Z. X., Tan, T. W., & Svec, F. (2013). Preparation of porous styrenics-based monolithic layers for thin layer chromatography coupled with matrix-assisted laser-desorption/ionization time-of-flight mass spectrometric detection. *Journal of Chromatography A*, 1316, 154–159.
- Ma, G. F., & Chen, L. G. (2014). Development of magnetic molecularly imprinted polymers based on carbon nanotubes – Application for trace analysis of pyrethroids in fruit matrices. *Journal of Chromatography A*, 1329, 1–9.
- Marmé, N., Knemeyer, J. P., Sauer, M., & Wolfrum, J. (2003). Inter- and intramolecular fluorescence quenching of organic dyes by tryptophan. *Bioconjugate Chemistry*, 14, 1133–1139.
- Masqueé, N., Marceé, R. M., & Borrull, F. (2001). Molecularly imprinted polymers: New tailor-made materials for selective solid-phase extraction. *TrAc Trends in Analytical Chemistry*, 20(9), 477–486.
- Ng, S. M., & Narayanaswamy, R. (2006). Fluorescence sensor using a molecularly imprinted polymer as a recognition receptor for the detection of aluminium ions in aqueous media. *Analytical and Bioanalytical Chemistry*, 386, 1235–1244.
- Pan, J. M., Xu, L. C., Dai, J. D., Li, X. X., Hang, H., Huo, P. W., et al. (2011). Magnetic molecularly imprinted polymers based on attapulgite/Fe₃O₄ particles for the selective recognition of 2,4-dichlorophenol. *Chemical Engineering Journal*, 174, 68–75.
- Piletsky, S. A., Piletska, E. V., Chen, B. N., Karim, K., Weston, D., Barrett, G., et al. (2000). Chemical grafting of molecularly imprinted homopolymers to the surface of microplates. Application of artificial adrenergic receptor in enzyme-linked assay for α -agonists determination. *Analytical Chemistry*, 72, 4381–4385.
- Shi, X. Z., Liu, J. H., Sun, A. L., Li, D. X., & Chen, J. (2012). Group-selective enrichment and determination of pyrethroid insecticides in aquaculture seawater via molecularly imprinted solid phase extraction coupled with gas chromatography-electron capture detection. *Journal of Chromatography A*, 1227, 60–66.
- Ware, W. R. (1962). Oxygen quenching of fluorescence solution: An experimental study of the diffusion process. *Journal of Physical Chemistry*, 66, 455–458.
- Ye, L., & Mosbach, K. (2008). Molecular imprinting: Synthetic materials as substitutes for biological antibodies and receptors. *Chemistry of Materials*, 20, 859–868.